MITSUBISHI ELECTRIC RESEARCH LABORATORIES
https://www.merl.com

Nonlinear Model Predictive Control for High-Thrust Geostationary Station Keeping using Averaged Dynamics

Pavlasek, Natalia; Acikmese, Behcet; Di Cairano, Stefano; Weiss, Avishai

TR2026-117 August 27, 2026

Abstract

Sequential convex programming (SCP) shows promise for fuel-optimal sparse control of high-thrust satellites in geostationary earth orbit (GEO), but is highly vulnerable to converge to local minima in the neighborhood of an initial guess. In particular, when optimizing for the time at which to perform a maneuver, these algorithms tend to find solutions within a few hours of the times at which they are initialized. In this work, we propose an algorithm that relies on averaged dynamics to form a proxy system with fewer nonconvexities than the true system. We use a consensus-based optimization framework to reach a consensus between the average and the true system, enabling the SCP to explore more of the solution space and enabling larger deviations of the converged solution from the initial guess. We demonstrate the performance of the proposed method against that of standard SCP on a problem in which the goal is to extend the time between east-west station-keeping maneuvers for a GEO satellite. Simulations are performed using NASA's General Mission Analysis Tool, a high-fidelity space mission simulator.

World Congress of the International Federation of Automatic Control (IFAC) 2026

Mitsubishi Electric Research Laboratories, Inc.
201 Broadway, Cambridge, Massachusetts 02139

Nonlinear Model Predictive Control for High-Thrust Geostationary Station Keeping using Averaged Dynamics

Natalia Pavlasek * **Behçet Açıkmeşe** * **Stefano Di Cairano** ** **Avishai Weiss** **

* *University of Washington, Seattle, WA 98195 USA (e-mail: {pavlasek, behcet}@uw.edu)*
** *Mitsubishi Electric Research Laboratories, Cambridge, MA 02139 USA (e-mail: {dicairano, weiss}@merl.com)*

Abstract: Sequential convex programming (SCP) shows promise for fuel-optimal sparse control of high-thrust satellites in geostationary earth orbit (GEO), but is highly vulnerable to converge to local minima in the neighborhood of an initial guess. In particular, when optimizing for the time at which to perform a maneuver, these algorithms tend to find solutions within a few hours of the times at which they are initialized. In this work, we propose an algorithm that relies on averaged dynamics to form a proxy system with fewer nonconvexities than the true system. We use a consensus-based optimization framework to reach a consensus between the average and the true system, enabling the SCP to explore more of the solution space and enabling larger deviations of the converged solution from the initial guess. We demonstrate the performance of the proposed method against that of standard SCP on a problem in which the goal is to extend the time between east-west station-keeping maneuvers for a GEO satellite. Simulations are performed using NASA's General Mission Analysis Tool, a high-fidelity space mission simulator.

Keywords: Spacecraft Control, Station Keeping, Nonlinear MPC, Sequential Convex Programming, Averaging

1. INTRODUCTION

Satellites in geostationary earth orbit (GEO) must maintain their position within an allotted station-keeping window. Despite the recent adoption of low-thrust electric propulsion, most active GEO satellites are equipped with high-thrust chemical propulsion systems. Since mission operations must generally be suspended during orbital maintenance, maximizing the time between such station-keeping maneuvers is often a key requirement.

Recent advances in trajectory optimization have enabled its use for high-thrust GEO station keeping (Pavlasek et al. (2025); de Bruijn et al. (2016)). Despite these advances (Elango et al. (2025); Lin et al. (2014); Malyuta et al. (2019); Kamath et al. (2023); Szmuk et al. (2020); Gazzino et al. (2017)), convex-optimization-based trajectory generation methods such as SCP rely on linearized models and yield locally optimal solutions. For systems with highly nonconvex dynamics such as satellites in orbit subject to disturbances, this assumption makes their solutions highly sensitive to local minima.

Satellites in orbit exhibit both short-period and long-period modes. Mean orbital elements have been used to model average long-term orbital motion by removing short-period variations (Gurfil (2004); Schaub et al. (2000)), but generally impose limitations on the perturbations that can be captured. A related concept of averaged dynamics (Sanders et al. (2007); Khalil (2002)) has been used more generally in the context of trajectory optimization (Harzer et al. (2025)) and dynamics integration (Calvo et al. (2011); Petzold et al. (1997)) for highly-oscillatory systems. These methods generally require sampling the dynamics at points at which the states of the average and true systems coincide.

Considering the average long-term orbital motion of a satellite reduces the nonconvexity of the trajectory optimization problem, but lacks the accuracy of the true system. We seek to combine the smoothness of the average system with the accuracy of the true system. Operator splitting has been proposed to form a consensus among agents solving slightly different trajectory optimization problems in Ganiban et al. (2025); Sindhwani et al. (2017). The use of operator splitting within SCP was shown to promote exploration within the sequential convex programming framework and to find solutions outside of the neighborhoods of any of the individual agents.

In this work, we propose an operator splitting framework that uses averaged dynamics to form a proxy system with fewer nonconvexities than the true system for maximizing time between station keeping maneuvers for GEO satellites. Preliminary work in Pavlasek et al. (2025) considered the use of a nonlinear model predictive control (NMPC) policy for station keeping under high-thrust impulsive control. We extend this work by proposing a numerical averaging method to capture the slow-changing mode of the highly oscillatory system over periods of several weeks without sacrificing model fidelity. Considering averaged dynamics enables larger variation of the maneuver application time from the initialization by mitigating the impact of local minima. We additionally consider the true system to capture local behavior, which is influenced by both the high-frequency oscillations and the slow-changing mode. We treat the solutions to the average problem and the true problem as agents, driven to a consensus on maneuver-application time using an operator-splitting framework. We compare the proposed method to a standard SCP algorithm and show that averaging leads to longer time between maneuvers.

The remainder of this paper is organized as follows. Section 2 introduces the problem and the concepts used in the proposed formulation. The proposed method is presented in Section 3, and results are provided in Section 4. Finally, concluding remarks are given in Section 5.

2. PROBLEM MODELING AND PRELIMINARIES

The following notation is used throughout this work. The vector $\underset{\rightarrow}{r}$ resolved in frame $\mathcal{F}_A$, defined by three orthonormal basis vectors $\{\underset{\rightarrow}{A}_1, \underset{\rightarrow}{A}_2, \underset{\rightarrow}{A}_3\}$, is denoted by $\mathbf{r}_A$. The vector describing the position of point c relative to point d is denoted by $\underset{\rightarrow}{r}^{\mathrm{cd}}$. The time derivative of $\underset{\rightarrow}{r}^{\mathrm{cd}}$ with respect to frame A is denoted $\underset{\rightarrow}{v}^{\mathrm{cd}/A}$. We use $\mathbf{e}^{\square}$ to denote a row vector with ones in the entries corresponding to the $\square$ indices of a vector, and zeros everywhere else. We denote the number of elements in vector $\mathbf{z}$ by $n_{\mathbf{z}}$. Finally, we use the shorthand $[K]$ to denote the set $\{0, \ldots, K\}$.

2.1 Satellite model

Consider a satellite in GEO. Its position vector relative to reference point ℓ that moves along a nominal Keplerian GEO is expressed as

$$\underset{\rightarrow}{r}^{\mathrm{s}\ell} = \delta x \underset{\rightarrow}{H_1} + \delta y \underset{\rightarrow}{H_2} + \delta z \underset{\rightarrow}{H_3}, \tag{1}$$

where s is a point at the center of mass of the satellite, δx, δy and δz are the components of the position vector of the satellite relative to the reference point ℓ, and $\mathcal{F}_H$ is Hill's frame. The position vector of the satellite with respect to an unforced particle located at the center of the Earth denoted by w is

$$\underset{\rightarrow}{r}^{\mathrm{sw}} = \underset{\rightarrow}{r}^{\ell\mathrm{w}} + \underset{\rightarrow}{r}^{\mathrm{s}\ell}. \tag{2}$$

We assume the existence of an inertial frame, denoted $\mathcal{F}_G$. The nonlinear equation of motion for the satellite relative to w with respect to $\mathcal{F}_G$ is

$$\underset{\rightarrow}{\ddot{r}}^{\mathrm{sw}}(t) = -\mu_{\mathrm{e}} \frac{\underset{\rightarrow}{r}^{\mathrm{sw}}(t)}{\left\| \underset{\rightarrow}{r}^{\mathrm{sw}}(t) \right\|_2^3} + \underset{\rightarrow\text{pert}}{a}^{\mathrm{sw}/G}(t) + \underset{\rightarrow\text{ctrl}}{a}^{\mathrm{sw}/G}(t), \tag{3}$$

where $\mu_{\mathrm{e}} \in \mathbb{R}$ is the standard gravitational parameter of the Earth, $\underset{\rightarrow\text{pert}}{a}^{\mathrm{sw}/G} : \mathbb{R}_+ \to \mathbb{R}^3$ is the acceleration induced by perturbing forces, and $\underset{\rightarrow\text{ctrl}}{a}^{\mathrm{sw}/G} : \mathbb{R}_+ \to \mathbb{R}^3$ is the input applied to the satellite. We consider perturbing accelerations from four sources: Sun and Moon third-body effects, solar radiation pressure, and Earth's non-Keplerian gravitational potential. See Pavlasek et al. (2025) for analytic expressions for the perturbing accelerations.

We consider satellites actuated by chemical thrusters, which operate every few weeks on the order of seconds and can effectively be modeled as impulsive accelerations, resulting in instantaneous velocity changes Δv. The acceleration input applied to the satellite is thus

$$\underset{\rightarrow\text{ctrl}}{a}^{\mathrm{sw}/G}(t) = \delta(t)\, \underset{\rightarrow}{u}(t), \tag{4}$$

where $\underset{\rightarrow}{u} : \mathbb{R}_+ \to \mathbb{R}^3$ is the control input, and $\delta(t)$ is the Dirac delta function. We further assume that the satellite is equipped with thrusters pointed in the velocity, or east-west (EW), direction and in the out-of-plane, or north-south (NS), direction. We assume that the satellite attitude control system is capable of orienting the satellite such that when a maneuver is applied, EW thrust is applied along $\underset{\rightarrow}{H_2}$ and NS thrust is applied along $\underset{\rightarrow}{H_3}$.

We take the state to be the position and the velocity of the satellite relative to the reference point ℓ with respect to $\mathcal{F}_H$ resolved in the spherical reference frame $\mathcal{F}_P$, where $\underset{\rightarrow}{P_1}$ is the radial direction, $\underset{\rightarrow}{P_2}$ is the azimuth angle, and $\underset{\rightarrow}{P_3}$ is the zenith angle. The satellite's state is thus

$$\mathbf{x} = \begin{bmatrix} r_{P_1}^{\mathrm{s}\ell} & r_{P_2}^{\mathrm{s}\ell} & r_{P_3}^{\mathrm{s}\ell} & v_{P_1}^{\mathrm{s}\ell/H} & v_{P_2}^{\mathrm{s}\ell/H} & v_{P_3}^{\mathrm{s}\ell/H} \end{bmatrix}^{\mathsf{T}}, \tag{5}$$

where $r_{P_i}^{\mathrm{s}\ell}(t)$ is the component of $r_P^{\mathrm{s}\ell}(t)$ along the P_i direction. The dynamics

$$\dot{\mathbf{x}}(t) = \mathbf{f}(t, \mathbf{x}, \mathbf{u}), \tag{6}$$

expressed in spherical coordinates are given in Willis et al. (2019) and follow from a rearrangement of (2) where $\underset{\rightarrow}{r}^{\ell\mathrm{w}}$ follows (3) with accelerations set to zero.

2.2 Station keeping

To maintain the satellites in their allotted GEO window, we impose a station-keeping constraint. The station-keeping constraint is expressed as bounds on components of the satellite state, $\mathbf{x}(t)$. Given the maximum deviation from the nominal longitude, $\bar{\theta} \in \mathbb{R}$, and the maximum deviation from the nominal latitude, $\bar{\phi} \in \mathbb{R}$, the station-keeping constraint is expressed as

$$\left| r_{P_2}^{\mathrm{s}\ell}(t) \right| \le \bar{\theta}, \quad \left| r_{P_3}^{\mathrm{s}\ell}(t) \right| \le \bar{\phi}. \tag{7}$$

While radial distance is not required to be constrained to satisfy typical GEO station-keeping requirements, it is implicitly constrained through coupling in the dynamics.

2.3 Sequential convex programming

We employ the prox-linear method (Drusvyatskiy and Lewis (2018); Szmuk et al. (2020); Elango et al. (2025)), to solve the nonconvex problem of finding a fuel-minimizing trajectory under the nonconvex dynamics given in (6).

Consider the nonconvex optimization problem

$$\min_{\mathbf{z} \in \mathcal{Z}} \; J(\mathbf{z}) \tag{8a}$$

$$\text{s.t. } \mathbf{g}(\mathbf{z}) \le 0, \tag{8b}$$

$$\mathbf{h}(\mathbf{z}) = 0, \tag{8c}$$

where $J : \mathbb{R}^{n_{\mathbf{z}}} \to \mathbb{R}$ is the objective function, $\mathcal{Z} \subset \mathbb{R}^{n_{\mathbf{z}}}$ is a convex set, and

$$\mathbf{g} = \begin{bmatrix} g_1(\mathbf{z}) & \cdots & g_{n_{\mathbf{g}}}(\mathbf{z}) \end{bmatrix}^{\mathsf{T}}, \; \mathbf{h} = \begin{bmatrix} h_1(\mathbf{z}) & \cdots & h_{n_{\mathbf{h}}}(\mathbf{z}) \end{bmatrix}^{\mathsf{T}}, \tag{9}$$

where $g_i : \mathbb{R}^{n_\mathbf{z}} \to \mathbb{R}$, for $i \in \{0, \ldots, n_\mathbf{g}\}$ are nonconvex inequality constraints, $h_i : \mathbb{R}^{n_\mathbf{z}} \to \mathbb{R}$, for $i \in \{0, \ldots, n_\mathbf{h}\}$ are nonconvex equality constraints.

Given a function $\square : \mathbb{R}^{n_\mathbf{x}} \to \mathbb{R}^{n_\square}$, we denote the function linearized about $\mathbf{z}^2$ as

$$\tilde{\square}(\mathbf{z}^1, \mathbf{z}^2) := \square(\mathbf{z}^2) + \nabla\square(\mathbf{z}^2)^\mathsf{T}(\mathbf{z}^1 - \mathbf{z}^2). \quad (10)$$

We define the cost for the penalty formulation of (8), linearized about $\mathbf{z}^{(j)}$ as

$$\Theta(\mathbf{z}, \mathbf{z}^{(j)}) := J(\mathbf{z}) + \left[\tilde{\mathbf{g}}(\mathbf{z}, \mathbf{z}^{(j)})\right]_+ + \left\|\tilde{\mathbf{h}}(\mathbf{z}, \mathbf{z}^{(j)})\right\|_1 \quad (11)$$

where $\mathbf{z}^{(j)} \in \mathbb{R}^{n_\mathbf{z}}$ is the state about which the problem is linearized, and $[\cdot]_+ = \max\{0, \cdot\}$.

We solve (8) using the iterative approach

$$\mathbf{z}^{(j+1)} \leftarrow \operatorname*{arg\,min}_{\mathbf{z} \in \mathcal{Z}} \Gamma(\mathbf{z}, \mathbf{z}^{(j)}) := \Theta(\mathbf{z}, \mathbf{z}^{(j)}) + \left\|\mathbf{z} - \mathbf{z}^{(j)}\right\|_2^2, \quad (12)$$

where $\mathbf{z}^{(0)}$ is the initial trajectory. The sequential minimization process is repeated until convergence of $\mathbf{z}^{(j+1)} - \mathbf{z}^{(j)}$ within tolerance ϵ^{tr}, and satisfaction of the linearized constraints satisfied within tolerance ϵ^{c}.

2.4 Trajectory optimization

In this section, we outline key elements required in our trajectory optimization formulation.

Continuous-time constraint satisfaction We use the isoperimetric constraint reformulation outlined in (Elango et al. (2025); Lin et al. (2014)) to impose continuous-time constraints as path constraints.

We introduce $y : \mathbb{R}_+ \to \mathbb{R}$ with dynamics and boundary value

$$\dot{y}(t) = \Lambda\left(t, \mathbf{x}(t), \mathbf{u}(t)\right), \quad (13a)$$

$$y(0) = y(t_f), \quad (13b)$$

where $\Lambda : \mathbb{R}_+ \times \mathbb{R}^{n_x} \times \mathbb{R}^{n_x} \to \mathbb{R}_+$ is defined as

$$\Lambda(t, \mathbf{x}, \mathbf{u}) = \sum_{i=1}^{n_\mathbf{g}} q_i(g_i(t, \mathbf{x}, \mathbf{u})) + \sum_{j=1}^{n_\mathbf{h}} p_j(h_j(t, \mathbf{x}, \mathbf{u})), \quad (14)$$

and $q_i : \mathbb{R} \to \mathbb{R}_+$, $i = \{1, \ldots, n_\mathbf{g}\}$, and $p_i : \mathbb{R} \to \mathbb{R}_+$, $i = \{1, \ldots, n_\mathbf{h}\}$ are exterior penalty functions. The variable y accumulates constraint violation.

Time dilation In the time-discretized OCP, impulsive control is achieved by applying control at the discrete time samples of the state trajectory. In order to allow maneuver-execution time to vary, we adopt a time dilated formulation of the dynamics Szmuk et al. (2020); Gazzino et al. (2017); Elango et al. (2025); Lin et al. (2014). Let t be a strictly increasing, continuously-differentiable mapping $t : [0, 1] \to \mathbb{R}_+$, with boundary conditions $t(0) = t_i$, $t(1) = t_f$. The derivative of the map is

$$s(\tau) = \frac{\mathrm{d}t(\tau)}{\mathrm{d}\tau}, \quad (15)$$

where $\tau \in [0, 1]$. We refer to s as the *dilation factor*.

Augmented Dynamics We define an augmented control input

$$\tilde{\mathbf{u}}(\tau) = \left[(\mathbf{u}(\tau))^\mathsf{T} \; s(\tau)\right]^\mathsf{T}. \quad (16)$$

We augment the state with the constraint-violation-accumulation variable and time, and define an augmented state as

$$\tilde{\mathbf{x}}(\tau) = \left[(\mathbf{x}(\tau))^\mathsf{T} \; y(\tau) \; t(\tau)\right]^\mathsf{T}. \quad (17)$$

We denote a derivative with respect to τ as $\mathring{\square}$. The dynamics in (6) are expressed with respect to τ, as

$$\mathring{\tilde{\mathbf{x}}} = \frac{\mathrm{d}\tilde{\mathbf{x}}}{\mathrm{d}t}\frac{\mathrm{d}t(\tau)}{\mathrm{d}\tau} = \begin{bmatrix} \mathbf{f}\left(t(\tau), \mathbf{x}(\tau), \mathbf{u}(\tau)\right), \\ \Lambda\left(t, \mathbf{x}(t), \mathbf{u}(t)\right), \\ 1 \end{bmatrix} s(\tau), \quad (18a)$$

$$= \tilde{\mathbf{f}}\left(\tilde{\mathbf{x}}(\tau), \tilde{\mathbf{u}}(\tau)\right), \quad (18b)$$

where $\tilde{\mathbf{f}} : \mathbb{R}^{n_\mathbf{x}} \times \mathbb{R}_+ \times \mathbb{R}^{n_\mathbf{u}} \times \mathbb{R} \to \mathbb{R}^{n_\mathbf{x}+1}$.

The dynamics in (18b) are linearized and time discretized, resulting in

$$\tilde{\mathbf{x}}_{k+1} - \bar{\tilde{\mathbf{x}}}_{k+1} = \mathbf{A}_k\left(\tilde{\mathbf{x}}_k - \bar{\tilde{\mathbf{x}}}_k\right) + \mathbf{B}_k\left(\tilde{\mathbf{u}}_k - \tilde{\mathbf{u}}_k^{(j)}\right), \quad (19)$$

where $\bar{\tilde{\mathbf{x}}}_k = \bar{\tilde{\mathbf{x}}}_0 + \int_0^{\tau_k} \tilde{\mathbf{f}}\left(\tilde{\mathbf{x}}(0), \tilde{\mathbf{u}}^{(j)}(\tau)\right) \mathrm{d}\tau$.

2.5 Consensus optimization

We employ consensus optimization in the proposed framework to combine the average system and the true system. Consider the optimization problem

$$\min_{\mathbf{x}} \; f(\mathbf{x}) = \sum_{i=1}^{n_f} f_i(\mathbf{x}), \quad (20)$$

where $\mathbf{x} \in \mathbb{R}^{n_\mathbf{x}}$, $f : \mathbb{R}^{n_\mathbf{x}} \to \mathbb{R}$, and $f_i : \mathbb{R}^{n_\mathbf{x}} \to \mathbb{R}$ for $i = 1, \ldots, n_f$. Problem (20) can be expressed as

$$\min_{\{\mathbf{x}\}_{i=1}^{n_f}} \sum_{i=1}^{n_f} f_i(\mathbf{x}_i) \quad (21a)$$

$$\text{s.t. } \mathbf{x}_i - \mathbf{x}_j = 0, \; i, j \in [n_f], \; i \neq j, \quad (21b)$$

where $\mathbf{x}_i$ for $i \in [n_f]$, are introduced to enable splitting the additive objective $f(\mathbf{x})$. In this form, the problem is separable across the objectives $f_1(\mathbf{x}_1), \ldots, f_{n_f}(\mathbf{x}_{n_f})$. It can then be solved using the iterative approach (Boyd et al. (2011); Ganiban et al. (2025))

$$\mathbf{x}_i^{(j+1)} = \operatorname*{arg\,min}_{\mathbf{x}} f_i(\mathbf{x}) + \frac{\rho}{2}\left\|\mathbf{x} - \bar{\mathbf{x}}^{(j)} + \boldsymbol{\xi}^{(j)}\right\|_2^2, \; i \in [n_f]$$

$$\bar{\mathbf{x}}^{(j+1)} = \frac{1}{n_f}\sum_{i=1}^{n_f}\left(\mathbf{x}_i + \boldsymbol{\xi}_i^{(j)}\right)$$

$$\boldsymbol{\xi}_i^{(j+1)} = \boldsymbol{\xi}_i^{(j)} + \left(\mathbf{x}_i^{(j)} - \bar{\mathbf{x}}^{(j)}\right), \qquad i \in [n_f],$$

where $\boldsymbol{\xi}_i \in \mathbb{R}^{n_\mathbf{x}}$ are the dual variables of Problem (21), and $\rho \in \mathbb{R}_+$ is the consensus penalty parameter. The dual variables update drives the primal variables into consensus. The quadratic regularization drives the variables towards the average of the primal variables, while the primal variables also minimize each function $f_i(\mathbf{x}_i)$.

Within SCP, operator splitting can be used to coalesce trajectories found by solving slightly different optimization problems into a single trajectory (Ganiban et al. (2025); Sindhwani et al. (2017)).

We define the decision variable, $\mathbf{z}$ as

$$\mathbf{z} = \left[\mathbf{z}_1^\mathsf{T} \cdots \mathbf{z}_K^\mathsf{T}\right]^\mathsf{T}, \quad \mathbf{z}_k = \left[\mathbf{x}_k{}^\mathsf{T} \; \mathbf{u}_k{}^\mathsf{T}\right]^\mathsf{T}, \; k \in [K], \quad (23)$$

where for notational simplicity, we define $\mathbf{u}_K$ as a vector of zeros. The decision variable is partitioned into consensus

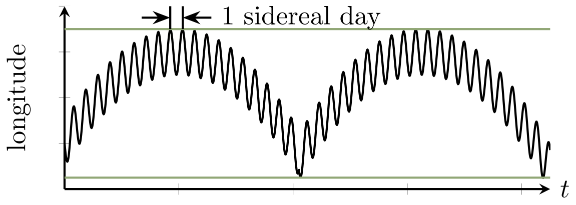

Fig. 1. Illustration of longitude over time for a typical GEO satellite.

components, $\mathbf{z}^c$, and free components, $\mathbf{z}^f$. The consensus components correspond to portions of the state for which all agents are driven to a common value, whereas the free components may vary across agents. We use $\boxplus$ to denote the concatenation of the consensus and free components of the state, such that $\mathbf{z} = \mathbf{z}^f \boxplus \mathbf{z}^c$.

Within SCP, each agent's trajectory is computed by solving a modified form of (12), namely

$$\mathbf{z}^{(j+1)} \leftarrow \underset{\mathbf{z}\in\mathcal{Z}}{\arg\min}\, \Gamma^c(\mathbf{z}, \mathbf{z}^{(j)}, \bar{\mathbf{z}}^{(j)}, \xi^{(j)}) := \Theta(\mathbf{z}, \mathbf{z}^{(j)}) + \left\|\mathbf{z}^f - \mathbf{z}^{f\,(j)}\right\|_2^2 + \frac{\rho}{2}\left\|\mathbf{z}^c - \bar{\mathbf{z}}^{(j)} + \xi^{(j)}\right\|_2^2. \tag{24}$$

3. STATION KEEPING USING AVERAGED DYNAMICS

SCP solutions are highly sensitive to the initial trajectory. In GEO station-keeping problems, this sensitivity may generate challenges due to the oscillatory nature of the dynamics, which introduces many local minima into the optimization landscape. SCP has been shown to effectively solve for maneuver application times and magnitudes that result in station-keeping window satisfaction (Pavlasek et al. (2025)). However, when optimizing for maneuver timing, the solution typically remains within one day of its initialization.

The longitude evolution of a satellite in GEO controlled with chemical thrust is illustrated in Fig. 1. The dynamics have two modes, with a high-frequency, small-amplitude mode induced by the orbital nature of the system, and a low-frequency mode caused by drift resulting from Earth's non-spherical shape (Larson and Wertz (1999)).

For satellites that must be taken offline during control application, it is advantageous to maximize time between maneuvers. The oscillatory behavior of the system makes optimizing for maneuver time challenging. To address this issue, we reduce the number of local minima by considering the averaged dynamics, which filter out high-frequency oscillations. For the purposes of this work, we focus on extending the time between EW maneuvers since NS maneuvers are typically performed with lower frequency.

In this section, we outline the proposed averaged dynamics SCP algorithm.

3.1 Averaged dynamics

Consider an agent with dynamics

$$\mathring{\tilde{\mathbf{x}}} = \tilde{\mathbf{f}}(\tilde{\mathbf{x}}(\tau), \tilde{\mathbf{u}}(\tau)). \tag{25}$$

We define an average agent as the system with dynamics

$$\mathring{\tilde{\mathbf{x}}}^{\mathrm{a}}(\tau) = \tilde{\mathbf{f}}^{\mathrm{a}}(\tilde{\mathbf{x}}(\tau), \tilde{\mathbf{u}}(\tau)) = \frac{1}{T}\int_{\tau-T/2}^{\tau+T/2} \tilde{\mathbf{f}}(\tilde{\mathbf{x}}(\tau'), \tilde{\mathbf{u}}(\tau'))\mathrm{d}\tau', \tag{26}$$

where $T \in \mathbb{R}_+$ is the period of the oscillations in the uniform-time space. The relationship between the period of oscillations in true time space, $T^t \in \mathbb{R}_+$, and T is

$$T = \frac{T^t}{s}, \tag{27}$$

where s is the dilation factor. In this work, the averaged dynamics cannot be expressed analytically due to the perturbations included in the dynamics model. Simplified perturbation models that can be averaged analytically do not capture the dynamics with sufficient accuracy for use over the time period we consider.

Time-discretizing dynamics typically entails numerically integrating the dynamics between subsequent sample times. Integrating (26) over $[\tau_k, \tau_{k+1}]$ necessitates solving nested integrals. We exploit the identity

$$\tilde{\mathbf{f}}^{\mathrm{a}}(\tilde{\mathbf{x}}(\tau), \tilde{\mathbf{u}}(\tau)) = \frac{1}{T}\int_{\tau-T/2}^{\tau+T/2} \tilde{\mathbf{f}}(\tilde{\mathbf{x}}(\tau'), \tilde{\mathbf{u}}(\tau'))\mathrm{d}\tau' \tag{28a}$$

$$= \frac{1}{T}\left(\tilde{\mathbf{x}}\left(\tau + \frac{T}{2}\right) - \tilde{\mathbf{x}}\left(\tau - \frac{T}{2}\right)\right), \tag{28b}$$

to avoid nested integration, which yields an exact and efficient implementation. This framework is illustrated in Fig. 2. The integrated state is the concatenation of the average state at the current time with the true state half a period ahead and the true state half a period behind the current time.

To solve a trajectory optimization problem using SCP, a discrete-time linear form of the dynamics is required. The state transition matrices of the average system are given by

$$\mathbf{A}^{\mathrm{a}}(\tau) = \frac{1}{T}\left(\mathbf{A}\left(\tau + \frac{T}{2}\right) - \mathbf{A}\left(\tau - \frac{T}{2}\right)\right), \tag{29a}$$

$$\mathbf{B}^{\mathrm{a}}(\tau) = \frac{1}{T}\left(\mathbf{B}\left(\tau + \frac{T}{2}\right) - \mathbf{B}\left(\tau - \frac{T}{2}\right)\right). \tag{29b}$$

To account for the fact that the average system has smaller magnitude than the true system since it neglects the high-frequency oscillations, the station-keeping constraint, enforced as a path constraint by integrating (13a), is tightened. The tightened constraint is computed using the mean magnitude of the oscillations, found by propagating the true oscillatory system.

3.2 Operator Splitting

The average system informs maneuver timing. Since the average system does not have knowledge of the local behavior of the system, we additionally use the true system to determine the precise maneuver-application time. Intuitively, the average system dictates the day on which to apply the maneuver, and the true system determines the time of day.

We treat the optimization problem as a consensus problem with two agents, which solve the true problem and the averaged problem, respectively.

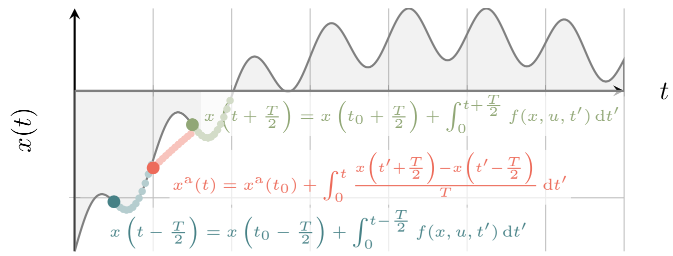

Fig. 2. Illustration of average integration. The state is integrated with a half-period lead (green) and a half-period lag (blue). The mean of the resulting states is integrated to compute the average state (red).

We define the average and true variables as

$$\mathbf{z}_k^{\mathrm{a}}=\left[(\tilde{\mathbf{x}}_k^{\mathrm{a}})^{\mathsf{T}}\,(\tilde{\mathbf{u}}_k^{\mathrm{a}})^{\mathsf{T}}\right]^{\mathsf{T}},\quad \mathbf{z}_k^{\mathrm{t}}=\left[(\tilde{\mathbf{x}}_k^{\mathrm{t}})^{\mathsf{T}}\,(\tilde{\mathbf{u}}_k^{\mathrm{t}})^{\mathsf{T}}\right]^{\mathsf{T}},\tag{30}$$

where $\tilde{\mathbf{x}}_k^{\mathrm{a}}$ and $\tilde{\mathbf{u}}_k^{\mathrm{a}}$ are the average augmented state and control at time t_k, and $\tilde{\mathbf{x}}_k^{\mathrm{t}}$ and $\tilde{\mathbf{u}}_k^{\mathrm{t}}$ are the augmented true state and control at time t_k.

A consensus is only formed over the time component of the variable. We have

$$\mathbf{z}^c=\mathbf{e}^t\mathbf{z},\quad \mathbf{z}^f=\mathbf{e}^{\neg t}\mathbf{z},\tag{31}$$

where $\mathbf{e}^{\neg t}=\neg\mathbf{e}^t$ extracts all states except those corresponding to t.

3.3 Averaged Dynamics SCP

At each SCP iteration, the true agent convex subproblem is solved. Forming a consensus between the average system and the true system perturbs the true system. The true system is very sensitive to the times at which maneuvers are applied. After the system is perturbed, a few SCP iterations are required to recover a good solution.

If an analytical model of the averaged dynamics were available, the true system would not need to be propagated to obtain the average system, and the sensitivity of the true system would not affect the average system.

The goal of the average agent is to maximize the time between maneuvers, and the goal of the true system is to find the local time at which to apply the maneuver. We therefore define a time-extension cost for the average problem. The costs $J(\mathbf{z})$ in (11) are

$$J(\mathbf{z}^{\mathrm{a}})=-\mathbf{e}^t z_k^{\mathrm{a}},\quad J(\mathbf{z}^{\mathrm{t}})=0,\tag{32}$$

for the average and true system, respectively.

The proposed SCP algorithm is outlined in Algorithm 1. We use MPC to determine optimal control inputs over a receding horizon, and to provide feedback to the system. For each MPC period, Algorithm 1 is used to solve for a trajectory over the planning period, T^{pp}. The dynamics are propagated using NASA's General Mission Analysis Tool (GMAT) for time $[t_i, t^{\mathrm{app}}]$, where $t^{\mathrm{app}}<t_f$ with the control inputs found by solving the optimal control problem. The state of the system at the end of the propagation becomes the initial trajectory $\mathbf{z}^0$ for the next MPC period.

Remark 1. Since the average system is computed by integrating the true system, the average system is afflicted by the sensitivity of the true system. To mitigate this, the convex subproblem for the average system is only computed once the true system has converged below a specified tolerance.

Algorithm 1: SCP with averaged dynamics.

while $j\le j^{\max}$ *and* $\left\|z^{(j+1)}-z^{(j)}\right\|>\epsilon$ **do**
  $\mathbf{z}^{\mathrm{t}(j+1)}\leftarrow\arg\min_{\mathbf{z}^{\mathrm{t}}\in\mathcal{Z}^{\mathrm{t}}}\Gamma^c(\mathbf{z}^{\mathrm{t}},\mathbf{z}^{\mathrm{t}(j)},\bar{\mathbf{z}}^{(j)},\boldsymbol{\xi}^{\mathrm{t}(j)})$
  if $\left\|\mathbf{z}^{\mathrm{t}(j)}-\mathbf{z}^{\mathrm{t}(j-1)}\right\|<\epsilon^{\mathrm{tr}'}$ **then**
    $\mathbf{z}^{\mathrm{a}(j+1)}\leftarrow\arg\min_{\mathbf{z}^{\mathrm{a}}\in\mathcal{Z}^{\mathrm{a}}}\Gamma^c(\mathbf{z}^{\mathrm{a}},\mathbf{z}^{\mathrm{a}(j)},\bar{\mathbf{z}}^{(j)},\boldsymbol{\xi}^{\mathrm{a}(j)})$
  end
  $\bar{\mathbf{z}}^{(j+1)}\leftarrow\frac{1}{2}\sum_{i\in\{\mathrm{a},\mathrm{t}\}}\left(\mathbf{z}^{c,i(j+1)}+\boldsymbol{\xi}^{i(j)}\right)$
  $\boldsymbol{\xi}^{i(j+1)}\leftarrow\boldsymbol{\xi}^{i(j)}+\left(\mathbf{z}^{c,i(j+1)}-\bar{\mathbf{z}}^{(j+1)}\right),\quad i\in\{\mathrm{a},\mathrm{t}\}$
  $j\leftarrow j+1$
end

Table 1. Parameter values used in simulation.

Parameter	Symbol	Value
Relectivity constant	c^{refl}	1.09
Sun-facing area	s_{facing}	50 m^2
Satellite mass	m_{s_i}	2500 kg
Max. deviation in longitude, tightened	$\bar{\theta}$	0.080°
Max. deviation in latitude, tightened	$\bar{\phi}$	0.095°
Isoperimetric constraint relaxation	ϵ^y	1×10^{-4}
Consensus penalty parameter	ρ	1×10^{1}
Period of the oscillations in true time	T^t	1 sidereal day
Initial time between maneuvers	T^{init}	Varies
Planning period	T^{pp}	$4\times T^{\mathrm{init}}$

4. GEO MANEUVER SPACING MAXIMIZATION

In this section, we demonstrate the performance of the proposed method, and compare our method to the SCP implementation from Pavlasek et al. (2025). We initialize the standard SCP method with 21, 23, and 25 days between EW maneuvers, and the average SCP method with 26 days between EW maneuvers. The maximum allowed deviation from the nominal latitude is 0.1° and from the nominal longitude is 0.0875°. To account for numerical errors and mismatch between our dynamic model and that of GMAT, we enforce tightened station-keeping window constraints within the SCP problem. This is in addition to the tightening discussed in Section 3.1 for the average agent. The parameters used within the simulation are given in Table 1.

Fig. 3 shows the longitude of the satellite over time for standard SCP initialized with maneuvers occurring 21 and 23 days apart, and for our proposed method. The horizontal lines correspond to the tightened EW boundaries of the station-keeping window. The vertical lines indicate the times at which EW control is applied. The mean time between maneuvers is given in Table 2. The average SCP solution occupies more of the station-keeping window than the standard SCP solutions. The mean times between maneuvers for standard SCP initialized with 21 and 23 days between maneuvers are 21.2 days and 23.2 days, respectively, indicating minor deviation from the initialization. In both cases, the solution is a local minimum in the neighborhood of the initial guess. When initialized with 25

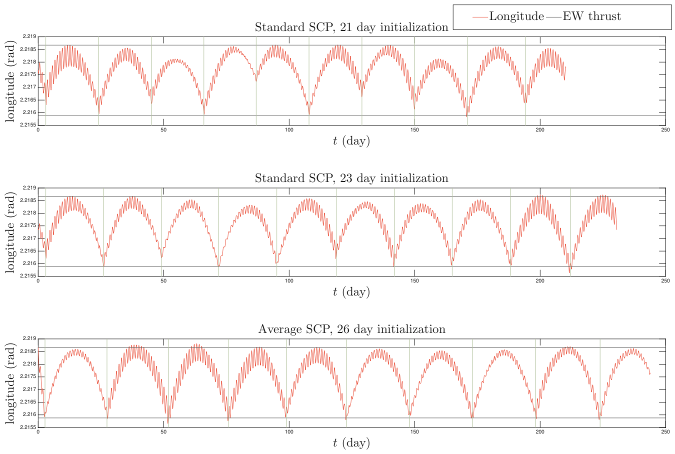

Fig. 3. Satellite longitude over time.

Table 2. Mean time between EW maneuvers.

Method	Init. time	Mean final time
Standard SCP	21 day	21.2226
Standard SCP	23 day	23.2164
Standard SCP	25 day	failed
Average SCP	26 day	**24.5727**

days between maneuvers, the standard SCP algorithm fails to converge. The average time between maneuvers using our proposed method is 24.6 days. This demonstrates that our method can attain longer uncontrolled time between maneuvers, and also shows that the solution is less constrained to the neighborhood of the initialization. Note that the constraints shown in Fig. 3 are tightened from the true constraint, making some violation acceptable.

5. CONCLUSION

A control strategy for incorporating averaged dynamics in SCP was presented. To mitigate the impact of local minima on the SCP solution to a highly nonconvex trajectory optimization problem, averaged dynamics were used compute a proxy problem with fewer local minima. The average and true system were treated as agents, driven to form a consensus on maneuver application time using an operator-splitting framework.

REFERENCES

Boyd, S., Parikh, N., Chu, E., Peleato, B., and Eckstein, J. (2011). Distributed optimization and statistical learning via the alternating direction method of multipliers. *Foundations and Trends in Machine Learning*, 3(1), 1–122.

Calvo, M., Chartier, P., Murua, A., and Sanz-Serna, J. (2011). Numerical stroboscopic averaging for ODEs and DAEs. *Applied Numerical Mathematics*, 61(10), 1077–1095.

de Bruijn, F.J., Theil, S., Choukroun, D., and Gill, E. (2016). Geostationary satellite station-keeping using convex optimization. *Journal of Guidance, Control, and Dynamics*, 39(3), 605–616.

Drusvyatskiy, D. and Lewis, A.S. (2018). Error bounds, quadratic growth, and linear convergence of proximal methods. *Mathematics of Operations Research*, 43(3), 919–948.

Elango, P., Luo, D., Kamath, A.G., Uzun, S., Kim, T., and Açıkmeşe, B. (2025). Continuous-time successive convexification for constrained trajectory optimization. *Automatica*, 180, 112464.

Ganiban, J., Pavlasek, N., and Açıkmeşe, B. (2025). A sequential operator-splitting framework for exploration of nonconvex trajectory optimization solution spaces.

Gazzino, C., Arzelier, D., Cerri, L., Losa, D., Louembet, C., and Pittet, C. (2017). Solving the minimum-fuel low-thrust geostationary station keeping problem via the switching systems theory.

Gurfil, P. (2004). Analysis of J2-perturbed motion using mean non-osculating orbital elements. *Celestial Mechanics and Dynamical Astronomy*, 90(3-4), 289–306.

Harzer, J., De Schutter, J., Rutquist, P., and Diehl, M. (2025). Implicit central difference approximations of averaged dynamics of highly oscillatory systems with applications to direct optimal control. *Optimal Control Applications and Methods*, 46(3), 1217–1234.

Kamath, A.G., Elango, P., Yu, Y., Mceowen, S., Chari, G.M., Carson III, J.M., and Açıkmeşe, B. (2023). Real-time sequential conic optimization for multi-phase rocket landing guidance. *IFAC-PapersOnLine*, 56(2), 3118–3125.

Khalil, H.K. (2002). *Nonlinear systems*, volume 3. Prentice hall Upper Saddle River, NJ.

Larson, W.J. and Wertz, J.R. (1999). Space mission analysis and design.

Lin, Q., Loxton, R., and Teo, K.L. (2014). The control parameterization method for nonlinear optimal control: A survey. *Journal of Industrial and Management Optimization*, 10(1), 275–309.

Malyuta, D., Reynolds, T., Szmuk, M., Mesbahi, M., Açıkmeşe, B., and Carson, J.M. (2019). Discretization performance and accuracy analysis for the rocket powered descent guidance problem. In *AIAA Scitech 2019 Forum*.

Pavlasek, N., Di Cairano, S., and Weiss, A. (2025). Geostationary satellite station keeping and collocation under high-thrust impulsive control. In *2025 American Control Conference (ACC)*, 4947–4953.

Petzold, L.R., Jay, L.O., and Yen, J. (1997). Numerical solution of highly oscillatory ordinary differential equations. *Acta numerica*, 6, 437–483.

Sanders, J.A., Verhulst, F., and Murdock, J. (2007). *Averaging methods in nonlinear dynamical systems*, volume 59. Springer.

Schaub, H., Vadali, S.R., Junkins, J.L., and Alfriend, K.T. (2000). Spacecraft formation flying control using mean orbit elements. *The Journal of the Astronautical Sciences*, 48(1), 69–87.

Sindhwani, V., Roelofs, R., and Kalakrishnan, M. (2017). Sequential operator splitting for constrained nonlinear optimal control. In *2017 American Control Conference (ACC)*, 4864–4871.

Szmuk, M., Reynolds, T.P., and Açıkmeşe, B. (2020). Successive convexification for real-time six-degree-of-freedom powered descent guidance with state-triggered constraints. *Journal of Guidance, Control, and Dynamics*, 43(8), 1399–1413.

Willis, M., Alfriend, K.T., and D'Amico, S. (2019). Second-order solution for relative motion on eccentric orbits in curvilinear coordinates.